



## Influence of Macro Synthetic Fibers on the Flexural Behavior of Reinforced Concrete Slabs with Opening

Rajai Z. Al-Rousan<sup>1\*</sup>

<sup>1</sup> Department of Civil Engineering, Jordan University of Science and Technology, Irbid, Jordan.

Received 14 June 2022; Revised 19 August 2022; Accepted 26 August 2022; Published 01 September 2022

### Abstract

In this study, the flexural behavior of one-way RC slabs after adding the macro discontinuous structural synthetic fiber (DSSF) under different opening sizes is investigated. Based on the previously conducted research, the 0.55 DSSF percentage was utilized since it was reported as the optimum value for enhancing the slab's performance. Moreover, further increases in the DSSF percentages proved to have the same improvement obtained by the 0.55%. Experimental testing was carried out on sixty-four one-way slabs under the effects of square opening existence (with or without), heat levels of 20, 200, 400, and 600 °C, and opening sizes of 100, 150, and 200 mm. The opening was created at the maximum bending moment region at the slab's center between the two loading points. For comparison purposes, the tested slabs were divided into main groups based on the DSSF existence. It was found that the resulted improvement by adding the DSSF material is affected by the size of the created opening. Furthermore, results revealed an increasing linear relationship between the applied load and the deflection and between the longitudinal concrete strain and the steel reinforcement. Besides, duplicating the opening size enhances the ductility index value by a maximum improvement percentage of 13% under an opening size ratio of less than 4.5%, while the improvement percentage becomes less under a further increase in the opening size ratio. Moreover, initial stiffness is more affected by increasing the temperature values twice those recorded for the yielding stiffness.

*Keywords:* Macro; Discontinuous Structural Synthetic Fiber; Flexural Behavior; Reinforced Concrete; Slab Opening.

### 1. Introduction

Structural stability and durability, including toughness and load-carrying capacity, are major concerns, especially after cracking, and many materials are used to improve these properties, such as steel, ceramics, glass, and synthetic fibers [1, 2]. Moreover, adding an appropriate quantity of fibers into concrete mixes reduces its brittle behavior, controls the onset of microcracking, and improves the concrete's tensile strength [3, 4]. Generally, the flexural concrete toughness and ductility are considerably affected by the fiber type, aspect ratio, and volume fraction. Literature has proved that a good performance could be obtained by adding steel fibers into the concrete mixture [5-7]. Therefore, researchers in the past ten years have focused on investigating the behavior of different fiber types other than steel [8-10], aiming to improve the slab's behavior through a feasible and applicable alternative that improves the concrete tensile strength and toughness, besides being chemically resistant to compensate for the corrosion problem [11-13]. DSSF fibers can be further used as a substitute for steel reinforcement. It has been proved that adding a 0.55% of DSSF improves the overall performance of the tested structural element, and this is related to its role in internal cracks stabilization [14].

Safety is a major concern during the design stage, which is affected by creating an opening within the structural element to accommodate different passing installations. Hanging slabs are commonly used for RC structures with

\* Corresponding author: [rzalrousan@just.edu.jo](mailto:rzalrousan@just.edu.jo)

<http://dx.doi.org/10.28991/CEJ-2022-08-09-016>



© 2022 by the authors. Licensee C.E.J, Tehran, Iran. This article is an open access article distributed under the terms and conditions of the Creative Commons Attribution (CC-BY) license (<http://creativecommons.org/licenses/by/4.0/>).

multiple floors or factories, and they contain different openings varying in size from large for elevators, stairways, and equipment to small for heat, plumbing, and electrical purposes. Structurally, opening of a small size affects the RC slab minorly, so the resultant additional stresses can be redistributed without significant degradation. Nevertheless, when a large opening is created, the concrete volume is reduced, and the reinforcement bars are interrupted, resulting in slab instability problems. Thus, the total capacity is reduced [15]. Moreover, the slab's behavior is also affected by the opening location for the probability of creating an opening in the maximum negative or positive moments to avoid losing the slab's capacity [16]. Therefore, according to the different international code provisions, the strip method is adopted to construct an RC slab with an opening regardless of size [17].

Creating an opening in a concrete slab minimizes the slab's performance in terms of ductility, energy absorption, and load-carrying capacity [15, 16]. Therefore, it is important to find an alternative material that could be used to substitute the effect of creating an opening within an RC structure and compensate for the steel reinforcement interruption, considering the size and location of the created opening. In the past ten years, researchers have shown that the DSSF fibers improve the concrete tensile strength and toughness, and it has been shown that short fibers can be used as an innovative material in concrete structures, which has a special design process mentioned in the national and international codes [18]. Furthermore, Sorelli et al. [19] stated that DSSF is the only substance that could be used in slabs on grades due to its high indeterminacy. In contrast, adding this new substance could improve the performance by using an optimum percentage reported as 0.55% [20, 21].

Lately, Hybrid Reinforced Concrete (HRC); a material made by combining DSSF and main reinforcing steel in a matrix of concrete, has been recognized as a method to optimize the structural performance and reduce the time and construction cost, and might minorly reduce the amount of the conventionally used steel reinforcement [22-24]. In contrast, using HRC increases the susceptibility to punching shear failure due to its large aspect ratio and low stiffness values [25]. Therefore, a combination of the randomly distributed short steel fibers and the conventionally used steel may be used to resist the high resultant tensile stresses that occur due to the highly induced deflections.

In recent years, several experimental research has been conducted to further investigate the feasibility of utilizing steel fibers to strengthen conventional concrete slabs. An experiment was carried out by Michels et al. [26] on concrete slabs with steel fibers. Test results revealed that when a 1.3% volume fraction is used, the possibility of punching failure is slightly reduced. Furthermore, a considerable effect on the slab thickness was observed in lowering the load-carrying capacity. Moreover, Michels et al. [27] suggested a guideline for designing structures with high-quality behavior using the Ultimate Limit States (ULS). Experimentation on a statically indeterminate slab was conducted by Pujadas et al. [28]. Slabs were strengthened with plastic polyolefin fibers of 9 kg/m<sup>3</sup> density. Results showed that the slab behaves more ductile under crack propagation due to the high-potential stress redistribution. Indeed, Destrée [29] investigated the behavior of typical slabs strengthened only with steel fibers. Therefore, modifications to the existing guidelines for slabs with steel fibers were recommended by RILEM, which overestimated the slab strength [30, 31].

High temperature severely deteriorates the overall behavior of concrete structures since it results in strength and stiffness characteristics degradation along with the induced high deformations [32, 33]. Different research stated that strengthening heat-damaged concrete elements with externally applied CFRP sheets generally helps restore the beam's flexural capacity depending on many factors such as the extent of damage and the amount of strengthening. Moreover, subjecting the damaged structure to cooling and heating cycles resulted in degrading its internal stability, which must be considered throughout the design process stage [34]. Furthermore, it is commonly known that concrete material losses its mechanical properties after exhibiting at a temperature greater than 500 °C, but it maintains its properties at temperature levels of 300 °C or less. The process of rapidly cooling degrades the concrete properties due to the temperature difference between the surface and the concrete core. The difference in temperature causes significantly tensile stresses to be produced and cracks within the concrete material are intensified causing concrete to expand and contract into aggregate and cement paste.

Many aspects affect the damage severity within concrete members, including the effect of cement type, size of the structure, aggregate type, moisture content, and environmental conditions such as the time of exposure, heating rate, cooling method, and the highest reached temperature [35]. Throughout the limited number of research available regarding the concrete slabs with opening, the inclusion of DSSF with a 0.55% ratio along with the main steel reinforcement is not common. It requires a further explanation for investigating the detailed behavior of the strengthened concrete. Therefore, this study aims to investigate the effectiveness of using the optimal DSSF ratio (0.55%) [36-38] at elevated temperature levels (20, 200, 400, and 600) °C on the flexural performance of one-way concrete slabs having a square opening with various sizes (100, 150, and 200) mm. Results are reported in terms of the failure mode, toughness, stiffness, load-deflection behavior, concrete and steel strains, and opening cracks. The proposed research methodology flowchart is illustrated in Figure 1.

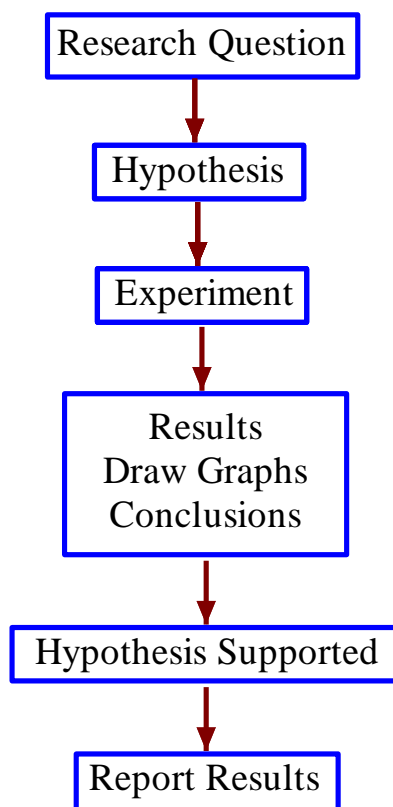


Figure 1. Research methodology flowchart

## 2. Research Significance

From the 70s to the last century, the idea of adding fibers into concrete mixes exists. As a result of their capability in improving the mechanical properties of concrete, ductility behavior, improving the concrete tensile strength, and controlling the onset of concrete cracking at the micro and macro levels. The major numbers of previously conducted research focus on the fiber's role in enhancing the structural performance of RC members. In contrast, limited research has been conducting the effectiveness of using macro synthetic fibers to improve the slab's performance, which composes the main motivation for this work. Creating an opening in an existing structure is necessary in some cases, such as elevators, stairways, and for passing installation purposes. Moreover, creating an opening reduces the overall performance of the RC slab, especially when it is located within the most critical region at the maximum positive or negative moment. The overall stability is significantly reduced, and the structure is weakened at this position due to concrete volume reduction and reinforcement interruption.

The slab's behavior is also affected by the presence of high-temperature levels since the mechanical characteristic of concrete is significantly reduced, such as its strength in compression and tension, volume stability, and modulus of elasticity, causing the slabs to lose its load-carrying capacity and failure might occur due to the additionally induced loads. However, the combined effect of the high temperature and opening existence on RC slabs' flexural performance has not yet been studied. Moreover, the effect of adding macro synthetic fibers (DSSF) is also examined. Therefore, two experimental sets were tested with or without DSSF substance for slabs having different opening sizes (100, 150, and 200) mm, under the effect of high-temperature levels.

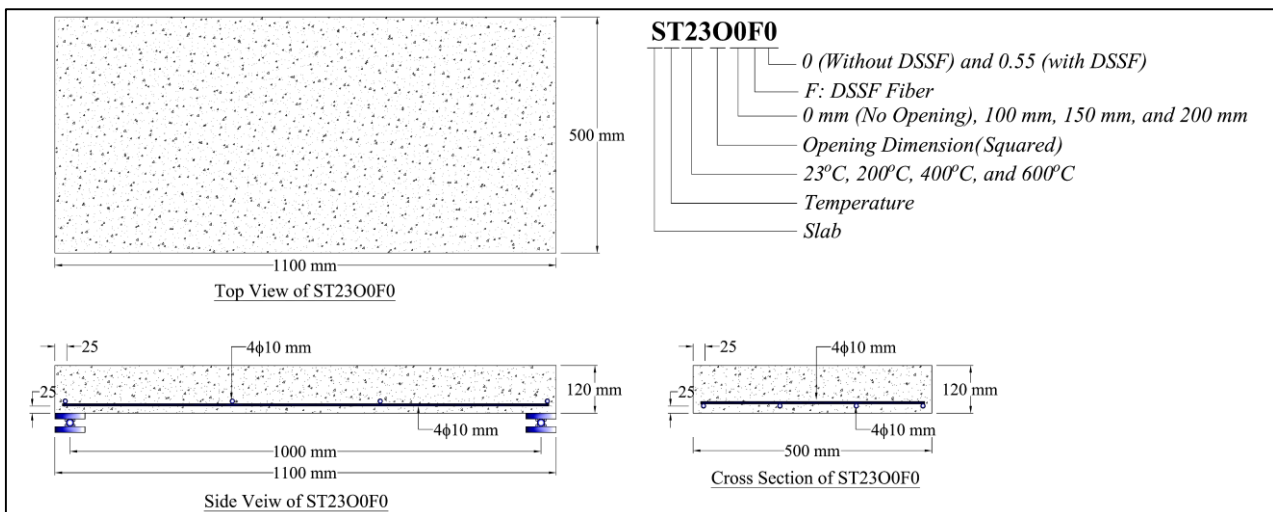
## 3. Experimental Program

### 3.1. Tested Slab Specimens

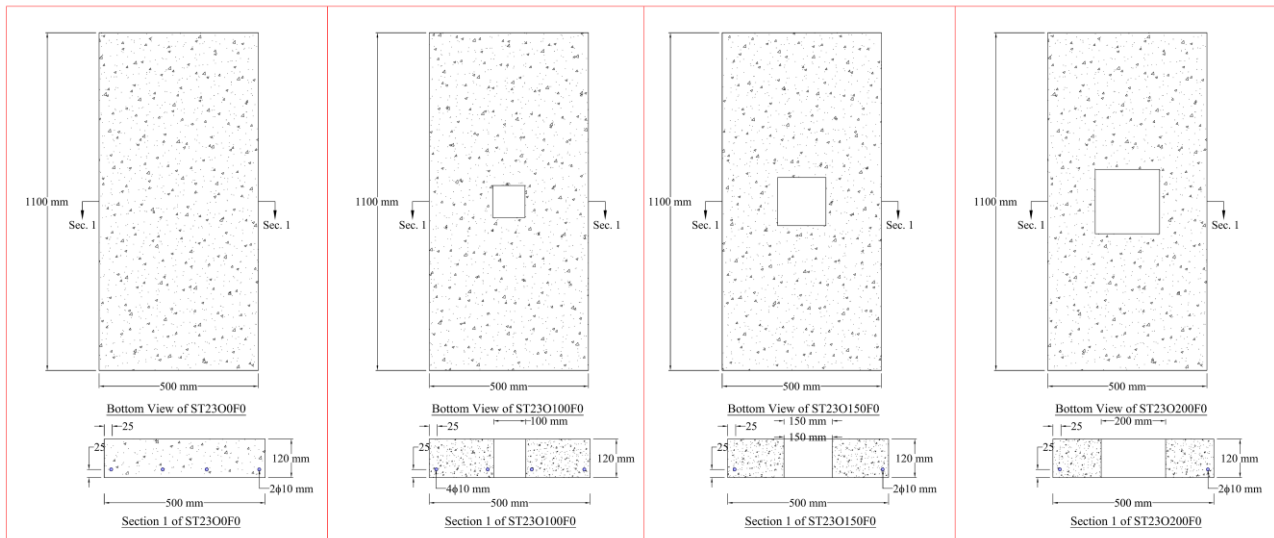
A total of (64) one-way slabs were tested for experimentation purposes. The specimens were simply supported and dimensioned as 1100 mm (long)  $\times$  500 mm (wide)  $\times$  120 mm (high). The parameters of the study consisted of the following: the ratio of added DSSF (0% and 0.55%), different temperatures (20, 200, 400, and 600)  $^{\circ}$ C, and the side length of the square-shaped opening (0 (without opening), 100, 150, and 200) mm, as shown in Table 1 and Figure 2-b. Therefore, the studied slab specimens consisted of two slab sets to investigate the effect of each parameter individually, as illustrated in Figure 2. Two steel pairs of 10mm diameter bars were installed longitudinally and transversely as the main reinforcement of the tested slabs. These bars have yield and ultimate strength values of 460 and 660 MPa, respectively. The main reinforcing steel at the opening location had been cut before the concrete was poured; later, a steel mesh was put in the wood molds after well-positioning the adequate spacers.

**Table 1. RC slabs details**

Slab designation	Temperature, °C	Opening dimension, mm	DSSF	Opening Ratio%
ST23O0F0	23	0 (No Opening)		None
ST200O0F0	200			
ST400O0F0	400			
ST600O0F0	600			
ST23O100F0	23	100	Without (None)	2%
ST200O100F0	200			
ST400O100F0	400			
ST600O100F0	600			
ST23O150F0	23	150		4.5%
ST200O150F0	200			
ST400O150F0	400			
ST600O150F0	600			
ST23O200F0	23	200		8%
ST200O200F0	200			
ST400O200F0	400			
ST600O200F0	600			
ST23O0F0.55	23	0 (No Opening)		None
ST200O0F0.55	200			
ST400O0F0.55	400			
ST600O0F0.55	600			
ST23O100F0.55	23	100	With DSSF (0.55%)	2%
ST200O100F0.55	200			
ST400O100F0.55	400			
ST600O100F0.55	600			
ST23O150F0.55	23	150		4.5%
ST200O150F0.55	200			
ST400O150F0.55	400			
ST600O150F0.55	600			
ST23O200F0.55	23	200		8%
ST200O200F0.55	200			
ST400O200F0.55	400			
ST600O200F0.55	600			



**(a) Reinforcement details and slab designs**



(b) Opening layout and details

Figure 2. RC slab a) reinforcement and b) opening layout and details

### 3.2. Concrete Mixture

Initially, the concrete mixtures were adjusted, and the utilized proportioning is illustrated in Table 2. The concrete mix contains the following proportions: 0.42:1.00:2.23:2.25 by the cement's weight ratio, knowing that the used cement was of Ordinary Type I Portland cement. Moreover, the utilized coarse aggregate was squashed limestone, having a 19.5 mm maximum aggregate size, 2.3% absorption, and 2.62 specific gravity values. Furthermore, the concrete mix contained fine aggregates with 1.9% absorption, 2.69 fineness modulus, and 2.65 specific gravity. The concrete mixes workability was enhanced by adding an amount of super-plasticizer, producing a nearly 75 mm slump value. The different aggregate grading is illustrated in Figure 3.

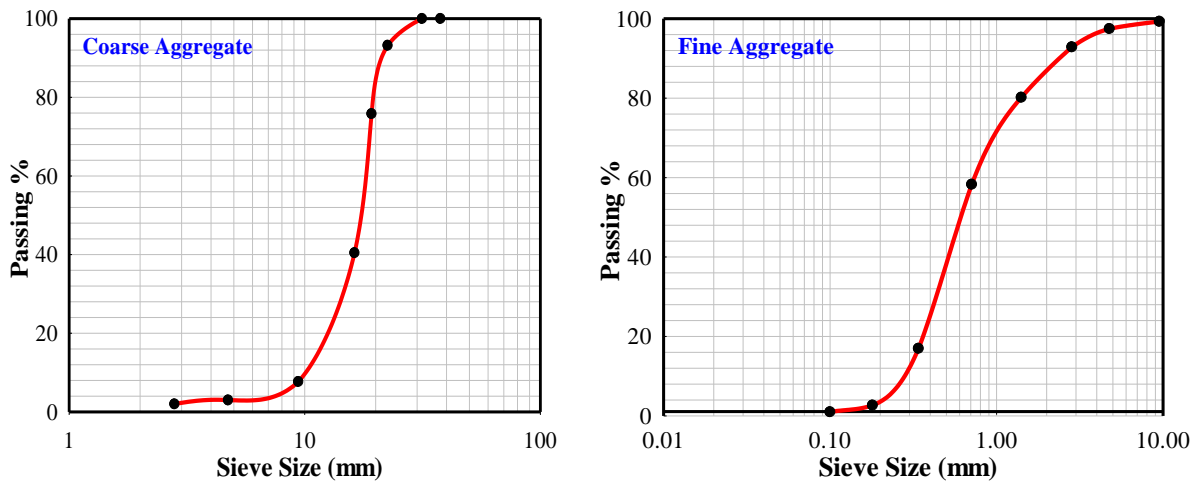


Figure 3. Aggregate grading curves

Table 2. Mix design proportions

Components	Quantity (kg/m <sup>3</sup> )
Cement	400
Water	168
w/c	0.42
Super- plasticizer	8
Coarse aggregate	890
Fine aggregate	900

The experimented slabs were prepared using a 0.15 m<sup>3</sup> capacity, tilting-type drum mixer (Figure 4). The preparation procedure started with soaking water into the internal surface of the utilized mixer. Then, a part of the water, along with the squashed aggregates of limestone, was put in the mixer while the mixer was kept rotating. After that, the rest of the

constituents (cement, water, and small-sized (fine) aggregates) were put moderately in the mixer. Later, the remaining portion of water was put in the mixing machine in addition to the super-plasticizer. The last step of preparing the concrete mixture was gradually distributing the required amount of DSSF over the prepared mix while keeping the mixing machine rotating. The right amount of DSSF to be added can be obtained from Table 3.



Figure 4. Mixing and casting of the RC slab

Table 3. The STRUX ® 90/40 manufactured of DSSF proportions

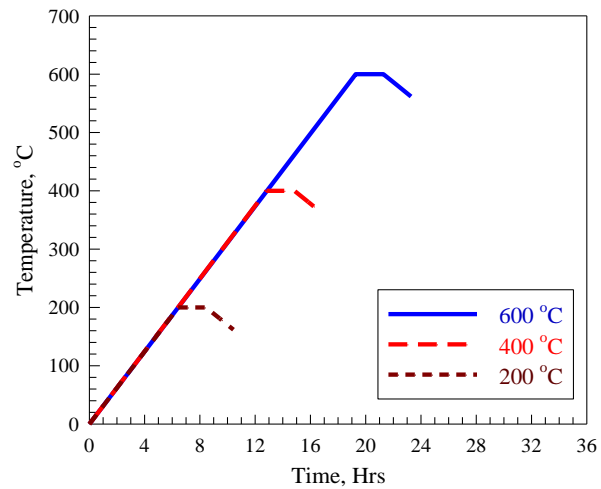
Property	Value
Length	40 mm
Aspect ratio	90
Absorption	None
Elastic stiffness	9.5 GPa
Tensile capacity	620 MPa
Melting point	160°C
Ignition point	590°C

Next, all of the constituents in the mixer were thoroughly mixed for (5) minutes to ensure the mix's homogeneity and the DSSF. After thoroughly mixing, wood molds were used to pour the concrete mix, internally dimensioned as 1100×500×120 mm; then, an electric vibrator was used to compel the molds. After being cast, the study samples were removed from the molds for a full day (24 hours); then, the samples were subject to curing by putting for four weeks (28 days) in a tank of water saturated with lime. At 28 days, the concrete cylinders -without DSSF (0%)- had a splitting tensile strength of 2.73 MPa and compressive strength of 36.4 MPa, while the ones with 0.55% of DSSF had a tensile strength of 3.10 MPa and compressive strength of 38.2 MPa. It has been noticed that adding DSSF will significantly improve the splitting tensile strength, as it increased that strength by almost 15%, whereas the DSSF resulted in a minor enhancement on the compressive strength, as the improvement percentage stays less than 5%.

### 3.3. Heat Treatment Method

An electric furnace was utilized to make the heat treatment, as shown in Figure 5. First, the concrete slabs were put in the furnace for (2) hours under a temperature ranging from 23 to 600 °C. Then, the heat-damaged slabs were left in the furnace for cooling down, with a 24°C/hour cooling rate, before they were wrapped with plastic wraps to avoid the potential of self-healing that could be resulted from the steel reinforcement. It is worth mentioning that the tested temperatures used in this work were (i.e., 23, 200, 400 and 600 °C) and were chosen to simulate the levels of temperature that could be encountered in actual residential structures when they undergo a fire situation for at least two hours. As

mentioned earlier, when concrete is exposed to extremely high temperatures, it encounters a considerable degradation in its load capacity and cracks propagation. Indeed, steel reinforcement characteristics are also degraded, which may result in the infeasibility of the repair options.



(a) The furnace

(b) The temperature history

**Figure 5. The (a) electric furnace and (b) time-temperature schedule**

### 3.4. Test Setup and Tools

The tested slabs were set up as simply supported with a 1000 mm length during the experiment. A specially designed frame was designed in the laboratory for this experiment, as shown in (Figure 6). A Hydraulic cylinder jacket was used to apply an intensive load (P) on a spread steel beam to obtain 400 mm-apart two points of loading (an area of a constant moment), aiming at obtaining an a/d (shear span/effective depth) ratio of 5. During the experiment, the following instruments were utilized: a strain gauge, a linear variable differential transformer (LVDT), and a load cell. To specify the precise position of measuring the cracks opening, a pilot sample with a square-shaped and another with a circular-shaped opening have experimented. LVDTs were put to measure: vertically-oriented displacements, tensile strains, compressive strains, and crack opening. Besides, a gauge to measure strains was placed right on the sample's compression side, while another gauge was placed in the samples themselves to record the steel strains before the samples were cast, as illustrated in Figure 6. In addition, the applied load was recorded using an embedded loading cell. Finally, results were gathered from the LVDTs and strain gauges using a data acquisition system.

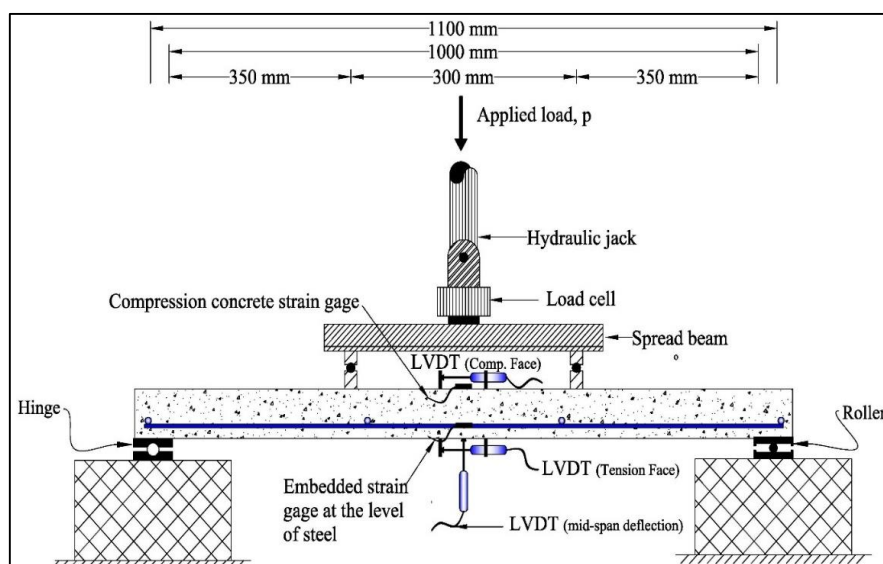


**Figure 6. Reinforcement detailing and test setup**

## 4. Results and Detailed Discussion

### 4.1. Concrete Strength

An overall of twelve concrete cylinders was experimentally tested to measure their modulus of elasticity, compressive, and tensile strength. Moreover, the tested cylinders were also divided into two sets depending on the DSSF

existence. Generally, the mechanical properties of concrete are degraded under the effect of high temperature. The ordinary concrete tested cylinder reported average compressive strength values of (36.4, 33.9, 22.6, and 16.0) MPa under the effect of the following temperatures (20, 200, 400, and 600) °C. Compared to the normal temperature level (20°C), it is observed that the elevated temperature resulted in compressive strength degradation percentages of (6.8, 37.8, and 56.0)% for the (200, 400, and 600) °C, respectively. Moreover, the tensile splitting strength was reported as (2.73, 2.61, 2.11, and 1.82) MPa, corresponding to a reduction percentage of (4.3, 22.8, and 33.2) % compared to normal temperature.

Concrete cylinders strengthened by 0.55% of DSSF reported compressive strength values of 38.4, 36.6, 26.4, and 19.5 MPa under the studied temperatures, and this corresponds to reduction percentages of 4.6, 31.1, and 49.1% compared to the DSSF concrete cylinder under normal conditions. Splitting tensile strength values under the different heat levels were (3.11, 3.0, 2.64, and 2.28) MPa with related reduction percentages of 3.8, 15.4, and 26.9%. Observing the experimental testing values shows that adding the DSSF material improves the concrete strength both in tension and compression. The average improvement percentages are 13% for compressive strength and 20% for splitting tensile strength. Amin et al. [39] studied the behavior after cracking a DSSF reinforced concrete using direct and indirect tensile testing techniques. An analytical model for predicting the residual tensile strength was proposed. Nevertheless, Mathews et al. [40] realized that the resulted degradation depends on the concrete compressive strength value. The mechanical properties of the macro synthetic fibers under elevated temperatures are investigated by Serafini et al. [41]. They reported that after the exposure to elevated temperature levels, the flexural strength is reduced by a value up to 85% due to the reinforcing mechanism degradation. In addition, Far and Nejadi [42] realized that adding DSSF improves the flexural performance of the concrete by 43.5%. On the other hand, stiffness capability is also improved by 25%.

#### 4.2. Cracking Patterns and Failure Modes

The different cracking patterns and failure modes were observed for all the tested specimens, as shown in Figures 7 and 8. A ductile failure type is observed for ordinary concrete slab where a crack is initiated at the loading location on the slab's bottom tensile side. Furthermore, additional flexural cracks appeared in the orthogonal direction upon load increasing until steel yielding occurred. After that, the concrete crushing within the maximum moment region in the middle of the tested slab. When an opening exists within the tested slab, the resulted flexural cracks longitudinally propagated on the slab's side surfaces and the inner opening faces. Moreover, cracks are widened after the steel yielding occurs within the opening region and are intensified until the concrete crushing occurs at the slab's compression face.



a) without opening



b) with squared opening of 100 mm×100 mm



c) with squared opening of 150 mm×150 mm



d) with squared opening of 200 mm×200 mm

Figure 7. Typical modes of failure of slabs (Room temperature) with different opening sizes



(a) 23°C



(b) 200°C



(c) 400°C



Figure 8. Typical modes of failure of slabs exposed to elevated temperatures with opening size of 200×200 mm

Generally, an opening within a slab plays a major role in reducing its cracking capability due to the reduced concrete volume and the interruption of the flexural reinforcement bars. Cracking within slab specimens of square opening in the maximum bending moment region undergoes crack propagation from the edge of the tension face. Then, cracks are increased within the opening region. Inspection of Figure 9 revealed that adding the DSSF material helps reduce the extent of cracking and its spreading by introducing internal stability into the structural element. Nevertheless, slabs with ordinary used concrete exhibit extensive cracks in their number and width. Therefore, the DSSF material helps provide the concrete with additional stability, which helps in improving the overall performance of the slabs under investigation. The sustained forces after cracking carried by the FRC depend on the type of the used fibers [43].

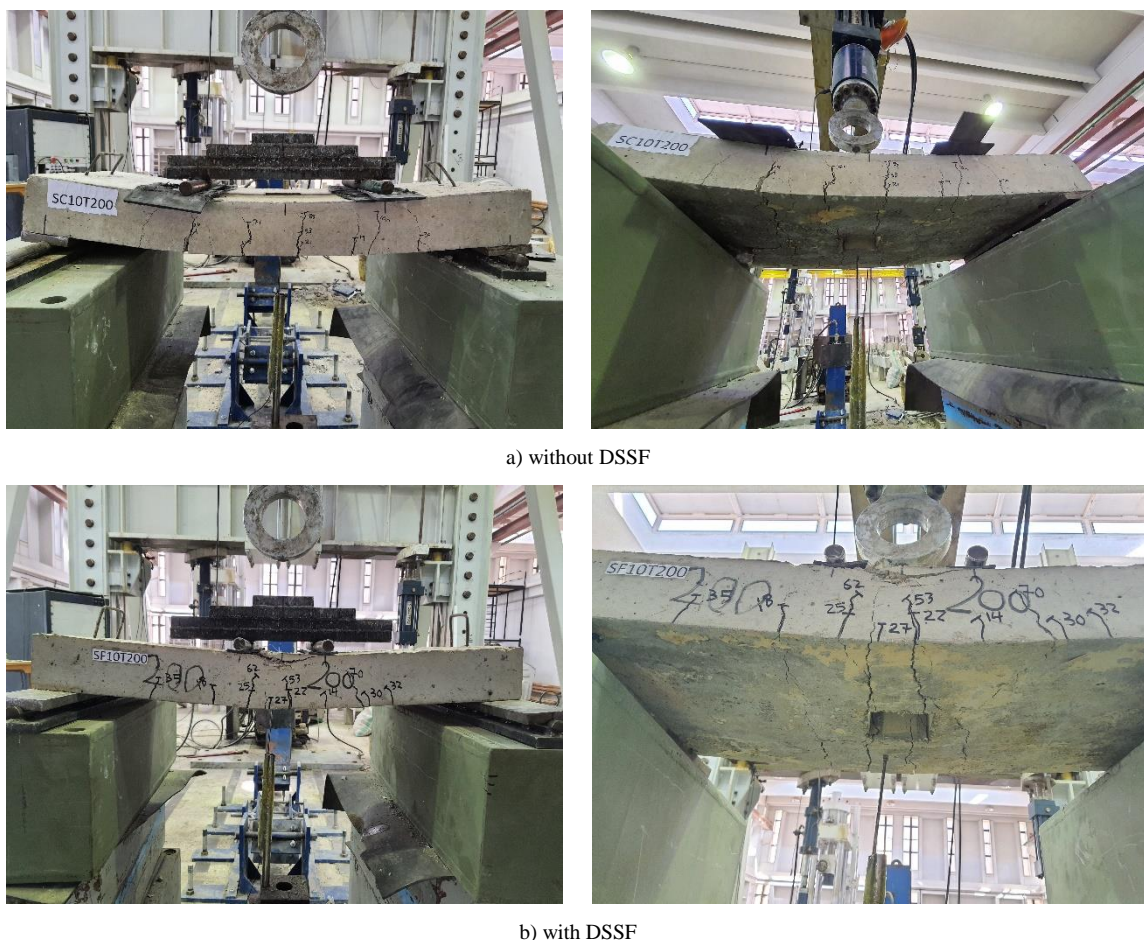


Figure 9. Impact of DSSF on the modes of failure of slabs with opening size of 100 mm×100 mm and exposed to 200°C

Table 4 shows the main obtained results at the different stages, including the cracking, yielding, and ultimate stages. Generally, it has been shown that slabs with an opening exhibited more degradation in their performance compared to those without an opening. This could be interpreted by the resulting stress concentration at the opening edge's locations and the crack intensification at the opening corners, as shown in Figure 7. However, it is observed that the feasibility of adding DSSF into the concrete mix is enhanced by increasing the opening ratio causing the slab's capacity to be

improved. The reported observation relies on the enhanced toughness and tensile characteristics after adding the DSSF into the concrete, causing the enhancement of the internal stability of the hybrid material.

**Table 4. Test results of all slabs**

Slab	$P_{cr}$ , kN	$\Delta_{cr}$ , mm	$P_y$ , kN	$\Delta_y$ , mm	$P_u$ , kN	$\Delta_u$ , mm	$\epsilon_s$ , $\mu\epsilon$	$\epsilon_c$ , $\mu\epsilon$	$w_{cr}$ , mm	$P_1$ @ $w_{cr}$ of 1mm, kN
ST23O0F0	23.6	1.14	60.4	4.05	72.6	41.44	4921	2418	3.96	67.0
ST200O0F0	21.3	1.52	54.8	5.43	66.3	38.73	4665	2404	3.38	61.0
ST400O0F0	18.9	1.57	48.7	5.35	59.5	36.25	4165	2277	3.26	54.5
ST600O0F0	16.7	1.92	43.6	7.14	53.4	28.19	3624	2107	2.40	48.8
ST23O100F0	23.0	1.31	54.1	4.01	66.8	44.92	6358	3725	4.29	56.4
ST200O100F0	20.5	1.74	48.6	5.57	60.5	41.86	6120	3662	3.65	50.9
ST400O100F0	17.5	1.74	43.0	5.54	53.8	39.03	5466	3380	3.51	45.2
ST600O100F0	15.3	2.09	36.7	7.21	48.0	30.27	4775	3223	2.57	39.5
ST23O150F0	22.4	1.76	46.0	4.61	57.4	53.60	6468	2522	5.12	42.7
ST200O150F0	19.9	2.35	41.3	6.58	51.8	49.83	6186	2498	4.35	38.5
ST400O150F0	17.4	2.40	35.4	6.23	45.9	46.31	5921	2419	4.17	33.6
ST600O150F0	15.2	2.91	30.4	8.24	40.7	35.82	5640	2462	3.04	29.4
ST23O200F0	21.8	2.78	31.8	5.15	40.9	62.89	8248	3393	6.01	23.6
ST200O200F0	19.1	3.67	28.1	7.29	36.9	58.32	6995	3252	5.09	21.1
ST400O200F0	16.4	3.63	24.6	6.97	32.5	54.01	6380	3002	4.86	18.6
ST600O200F0	14.1	4.41	21.6	9.63	28.8	41.67	6166	3098	3.54	16.4
ST23O0F0.55	29.4	1.46	69.2	4.81	82.8	48.90	4652	2787	4.67	76.6
ST200O0F0.55	26.4	1.96	62.6	6.66	75.5	45.70	6358	3725	3.99	69.6
ST400O0F0.55	22.8	1.96	55.9	6.36	67.8	42.77	6120	3662	3.85	62.3
ST600O0F0.55	19.9	2.37	47.9	8.31	60.9	33.26	5466	3380	2.83	54.8
ST23O100F0.55	27.3	1.60	64.9	5.31	76.1	53.00	4775	3223	5.06	65.8
ST200O100F0.55	24.2	2.12	57.5	6.98	69.0	49.40	4418	2748	4.31	59.0
ST400O100F0.55	20.8	2.13	51.0	6.91	61.4	46.06	4250	2738	4.15	52.4
ST600O100F0.55	18.1	2.56	43.9	8.88	54.7	35.72	3837	2731	3.04	46.0
ST23O150F0.55	26.3	2.14	52.8	5.63	65.4	63.25	5305	2214	6.04	48.8
ST200O150F0.55	23.2	2.83	47.1	7.78	59.1	58.80	5159	2160	5.13	43.9
ST400O150F0.55	20.7	2.95	40.1	7.44	52.3	54.64	4940	2157	4.92	38.2
ST600O150F0.55	18.1	3.58	34.4	9.77	46.4	42.27	4789	2250	3.59	33.4
ST23O200F0.55	23.9	3.21	36.0	6.16	46.7	74.22	5901	2787	7.09	26.9
ST200O200F0.55	20.8	4.18	32.0	8.68	42.0	68.82	5679	2740	6.01	24.0
ST400O200F0.55	17.7	4.15	27.8	8.33	37.1	63.73	5331	2718	5.74	21.1
ST600O200F0.55	15.1	4.90	24.4	11.27	32.8	49.17	5065	2683	4.18	18.6

Note:  $P_{cr}$ ,  $P_y$ , and  $P_u$  are the cracking, yield, and ultimate loads, respectively.  $\Delta_{cr}$ ,  $\Delta_y$ , and  $\Delta_u$  are the cracking, yield, and ultimate deflections, respectively.  $\epsilon_s$  is the steel reinforcement tensile strain,  $\epsilon_c$  is the concrete compressive strain,  $w_{cr}$  is the flexural crack width, and  $P_1$  is a load value corresponds to a crack width of 1 mm.

### 4.3. The Ultimate Load Capacity and Load-Deflection Behavior

The load-deflection behavior of the tested slabs is shown in Figure 10. Three different stages are observed; the first one starts from the point of loading up to the first appearing of a flexural crack, the second is from the point of cracking to the point of steel yielding, and finally, a plateau up to the failure point. Results are presented within two main groups depending on the opening and DSSF material under different temperature levels. Inspection of Table 4 shows the ultimate load and ultimate deflection values for all the tested slabs. It appears that increasing the temperature reduces the slab's load-carrying capacity. Moreover, the relationship between the opening size and the slab's capacity is also inversely proportional due to resulted reduction in the concrete volume and the amount of flexural reinforcement. The effect of different temperatures up to 300°C on the overall performance of FRC, including its residual compressive strength, cracking extent, and stress-strain curves, were investigated by Srikar et al. [44]. Different fiber dosages were tested under the effect of temperature, and it was concluded that the maximum improvement in the ultimate compressive strength was 15% for all cases.

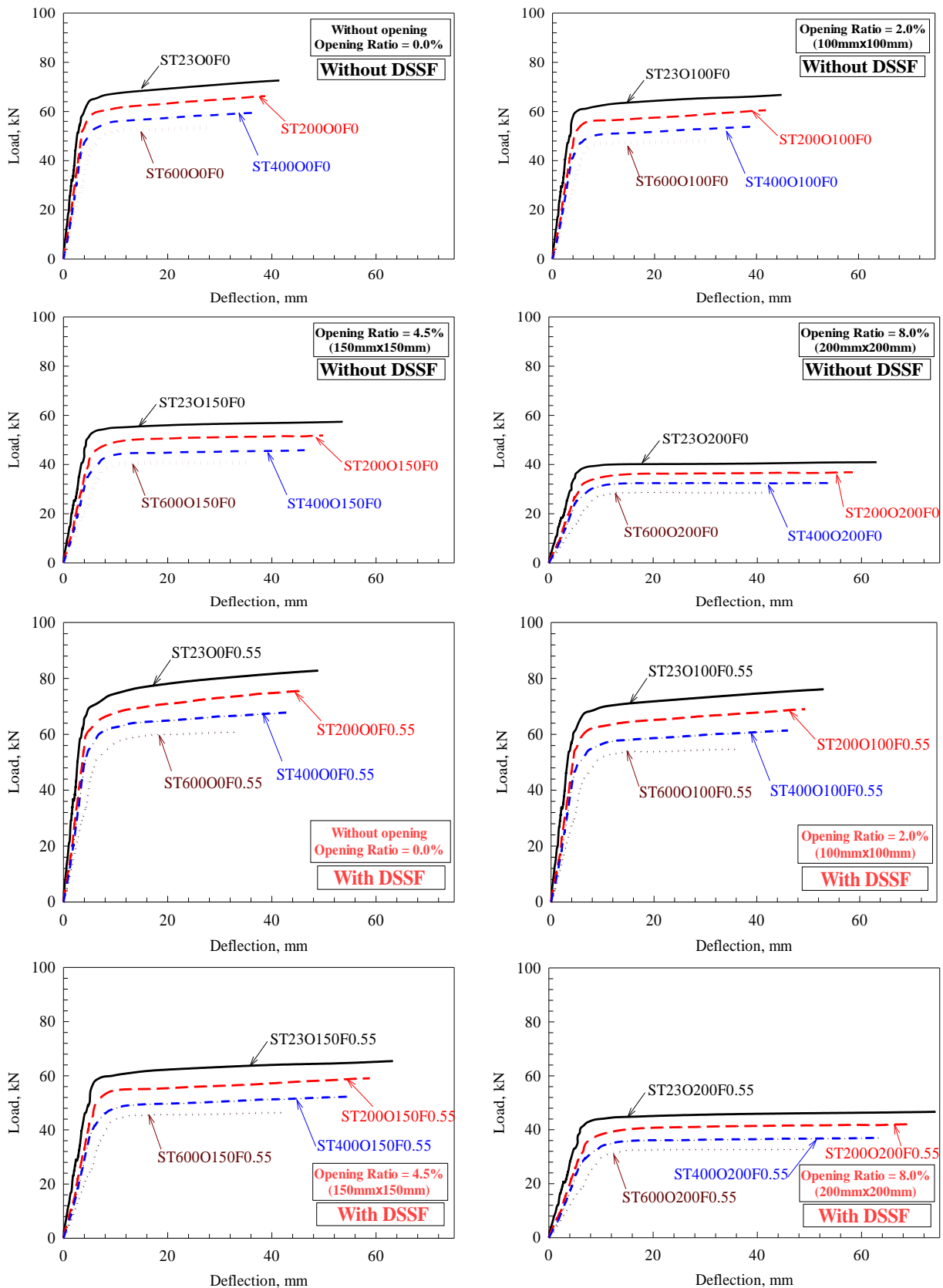
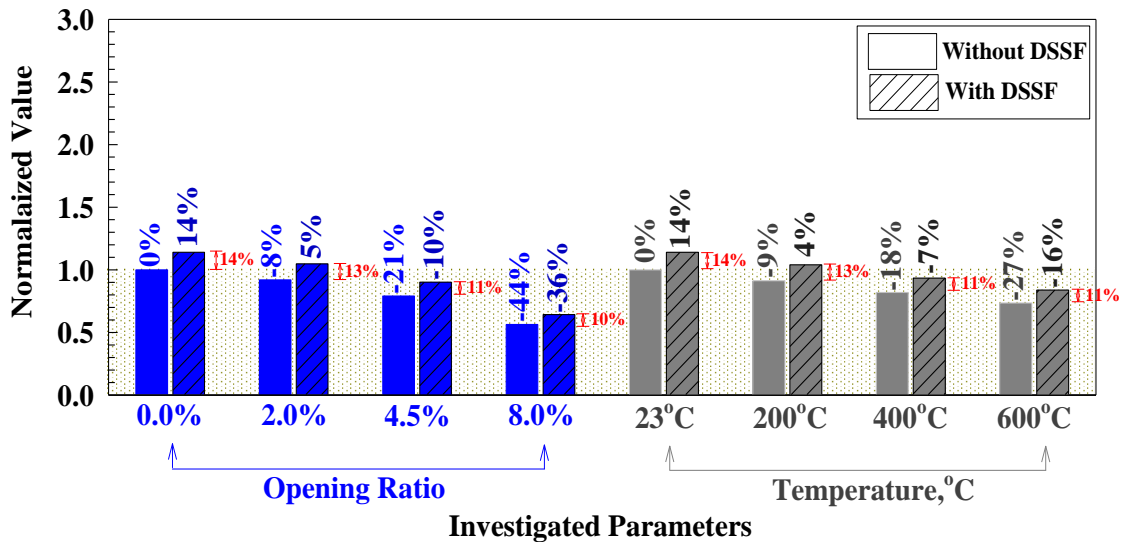


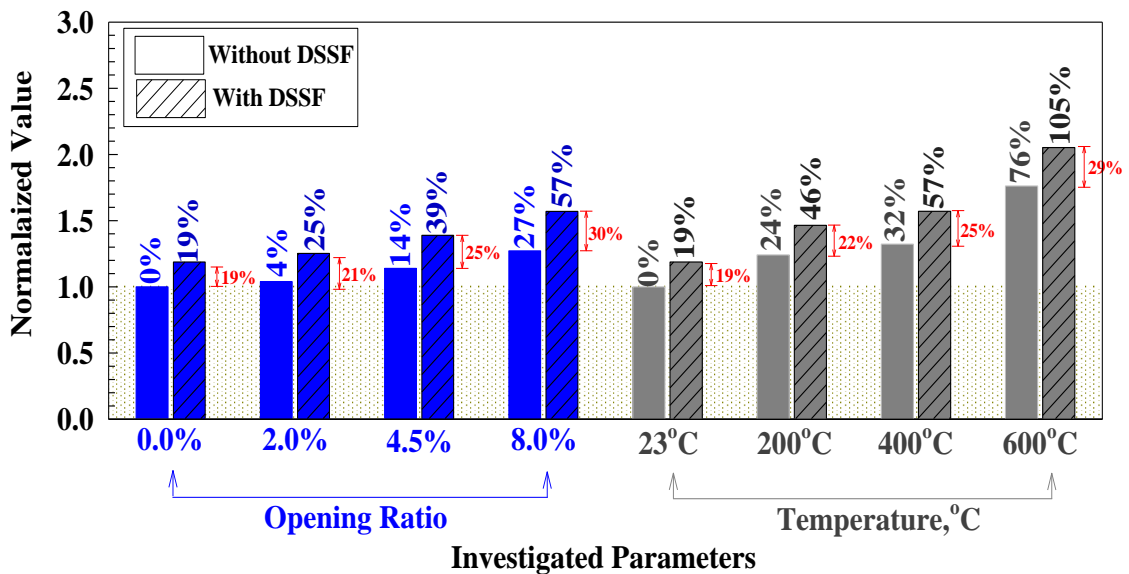
**Figure 10. Load versus deflection behavior for one-way slabs**

Analyzing the main finding shown in Figure 10 shows that adding DSSF material significantly enhances the ultimate strength, unlike those with ordinary concrete. Compared to (ST23O0F0) specimen; a slab without an opening or DSSF material, tested at room temperature, the ultimate load capacity was reduced by a percentage of 8, 21, and 44% for opening ratios 2.0, 4.5, and 8%, respectively. In addition, a reduction in the ultimate deflection values was reported where it varies between 4% for a 2% opening ratio and 27% for the 8% opening ratio specimens compared to the control slab.

Adding DSSF material proves to positively impact the flexural load-carrying capacity of slabs. It was found that an improvement percentage of 14 is recorded for a slab without an opening. Indeed, for an opening ratio of 2, 4.5, and 8, the improvement was 13, 11, and 10%, respectively. Thus, the ultimate capacity improvement percentage does not significantly affect by the presence of an opening. In contrast, the ultimate deflection improvement values were 19, 21, 25, and 30%. Thus, For DSSF strengthened slabs, increasing the opening ratio to twice the time causes the ultimate deflection to be increased by 4% on average. Furthermore, when a slab is exposed to high-temperature levels, its ultimate capacity is reduced to a value between 9 and 27%, only under the studied heat levels range. As a result, the ultimate deflection increases by 24 to 76%, as shown in Figure 11. Moreover, the inclusion of micro synthetic fibers into the concrete mix improves the ultimate load and deflection capabilities by (19 to 29) and (11 to 14) %, respectively.



(a) Failure load



(b) Failure deflection

Figure 11. Failure load and corresponding deflection behavior

#### 4.4. The Compressive strains in Concrete and Tensile Strains in Steel

Strain distribution values throughout the ST2300F0 model were recorded and presented in Figure 12 at different loading stages. The maximum obtained strain value was 150  $\mu\epsilon$  in both the concrete and steel materials as a result of the induced flexural cracks. Moreover, strain values during the second load-deflection stage reach 507 and 966  $\mu\epsilon$  for concrete and steel, respectively. This corresponds to 21% of the ultimate compressive strain for concrete and 42% of the steel yielding strain values. Upon the steel yielding occurs, the percentages increase to 34% for concrete and 100% for steel. During the final stage, a further increase in the steel strain is observed, which exceeds its yielding strain, while concrete strain does not exceed half the value of the crunching strain. Finally, after the failure of the reinforcing bars is reached, a rapid increase in the concrete strain is observed, and concrete crushing occurs while the steel strain reaches 214% of its yielding strain.

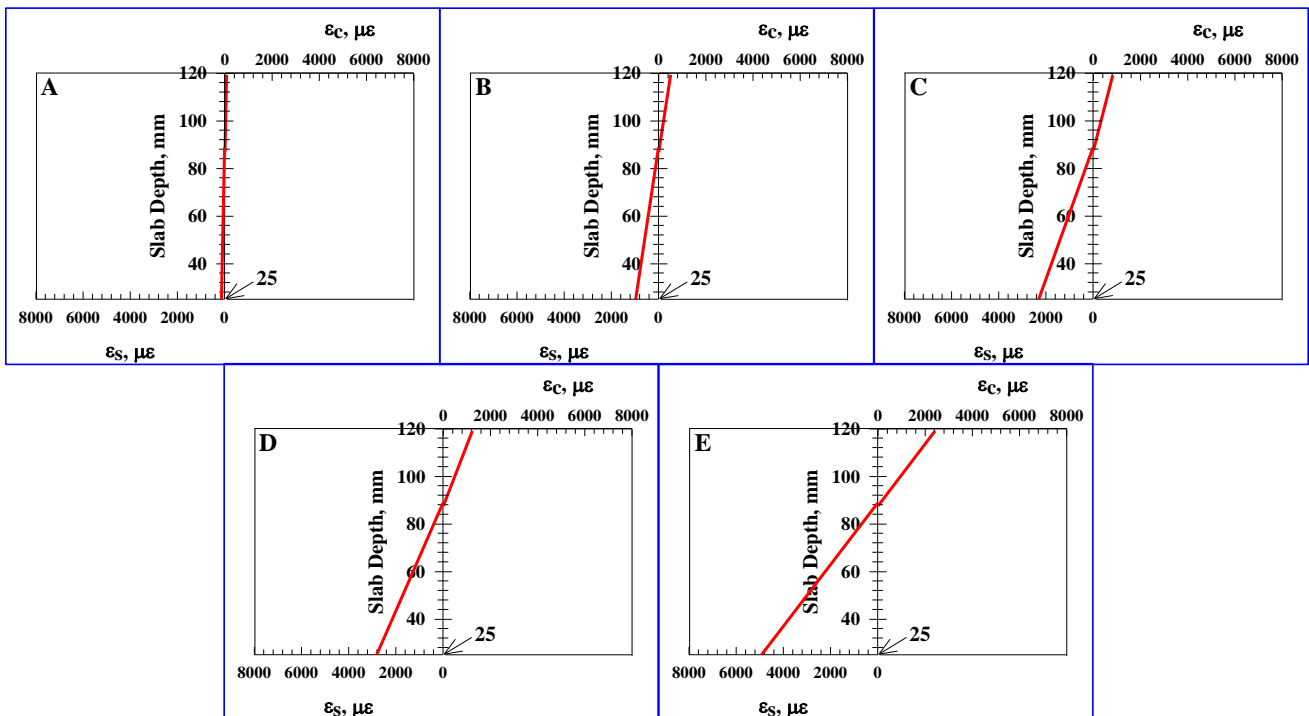
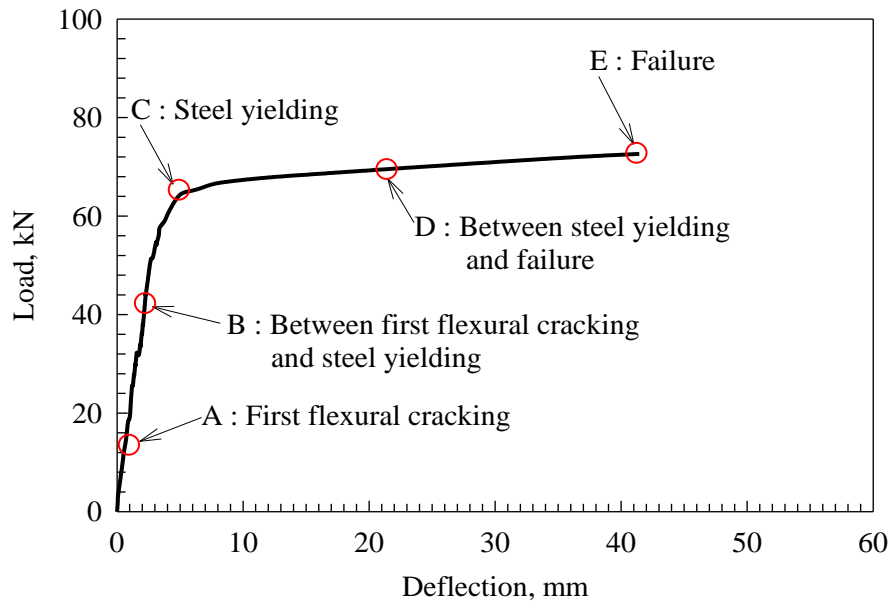


Figure 12. Distribution of strains at different depths along the ST2300F0

Table 4 records strain values for all the tested slabs for both concrete and steel materials. Observing the results revealed that increasing the opening size within a slab caused the strain value to be further increased for steel and concrete. However, strain values are decreased under the effect of increasing the temperature. The resulted degradation could explain this occurred under heat levels. Normalizing the obtained results with respect to the control slab specimen shows that a steel strain is significantly affected by the presence of opening and DSSF material. An improvement percentage of 29, 31, and 68% were observed for opening ratios of 2.0, 4.5, and 8.0%, respectively. Indeed, temperature increases the concrete strain values induced by 5, 15, and 26% for heat levels 200, 400, and 600°C, respectively. Furthermore, Bažant et al. [45] stated that the compressive stress-strain curves were observed at different temperatures (25, 200, 400, and 600)°C decreasing the concrete compressive strength by 9.2, 34.6, and 64.9% compared to concrete at 25°C. Moreover, Carnovale and Vecchio [43] stated that larger DSSF strains are required to produce the same stress levels induced by steel fibers. The observed phenomenon is related to a low modulus of elasticity compared to steel fibers.

#### 4.5. Elastic and Yielding Stiffness Characteristics

Two stiffness values were measured to represent the overall performance of the tested slabs in both the elastic and plastic deformations. The first measure is the initial or elastic stiffness calculated as slope of the load-deflection curve

from the loading up to the point of concrete cracking and it is defined mathematically as  $k_1 = P_{cr}/\Delta_{cr}$ . The second measure is the yielding stiffness, calculated as the slope of the second stage in the load-deflection curve. It is represented mathematically as follows:  $k_Y = P_Y/\Delta_Y$ . Inspection of Table 5 reveals that a significant reduction is observed under the effect of temperature increase, which was reduced from 10.23 to 3.95 kN/mm after it is heated at 600°C. Serafini et al. [41] realized that the observed reduction in the concrete elastic modulus was recorded as losses of 31.0, 87.6, and 96.6%.

**Table 5. Energy and ductility characteristics for the tested slabs**

Slab	Stiffness, kN/mm		Energy absorption, kN.mm		Ductility index	
	Elastic	Yielding	Yielding	At Failure	$\mu_A$	$\mu_{EA}$
ST23O0F0	20.76	14.91	203	2542	10.23	12.54
ST200O0F0	13.97	10.09	219	2087	7.13	9.52
ST400O0F0	12.01	9.09	269	1665	6.77	6.20
ST600O0F0	8.72	6.11	334	980	3.95	2.93
ST23O100F0	17.61	13.49	207	2557	11.20	12.33
ST200O100F0	11.80	8.72	218	2063	7.51	9.45
ST400O100F0	10.09	7.77	265	1626	7.05	6.14
ST600O100F0	7.30	5.09	348	928	4.20	2.67
ST23O150F0	12.69	9.96	217	2660	11.62	12.27
ST200O150F0	8.49	6.27	223	2148	7.57	9.65
ST400O150F0	7.25	5.68	270	1667	7.43	6.19
ST600O150F0	5.24	3.69	351	939	4.35	2.68
ST23O200F0	7.85	6.17	186	2238	12.21	12.06
ST200O200F0	5.22	3.86	188	1796	8.00	9.58
ST400O200F0	4.51	3.53	228	1396	7.75	6.12
ST600O200F0	3.19	2.25	289	770	4.33	2.66
ST23O0F0.55	20.06	14.40	271	3401	10.17	12.54
ST200O0F0.55	13.49	9.39	290	2787	6.86	9.60
ST400O0F0.55	11.60	8.79	361	2239	6.72	6.20
ST600O0F0.55	8.42	5.77	444	1316	4.00	2.96
ST23O100F0.55	17.01	12.21	272	3407	9.97	12.54
ST200O100F0.55	11.40	8.24	291	2771	7.07	9.52
ST400O100F0.55	9.75	7.39	352	2184	6.67	6.20
ST600O100F0.55	7.05	4.94	434	1274	4.02	2.93
ST23O150F0.55	12.26	9.39	286	3529	11.24	12.33
ST200O150F0.55	8.20	6.06	299	2829	7.56	9.45
ST400O150F0.55	7.00	5.39	360	2210	7.35	6.14
ST600O150F0.55	5.06	3.52	470	1254	4.33	2.67
ST23O200F0.55	7.45	5.85	244	2994	12.06	12.27
ST200O200F0.55	4.98	3.68	249	2405	7.93	9.65
ST400O200F0.55	4.25	3.33	300	1854	7.65	6.19
ST600O200F0.55	3.07	2.17	388	1038	4.36	2.68

The stiffness behavior of the one-way slabs is illustrated in Figure 13 normalized with respect to the control specimen. For the studied temperatures, the slab's initial stiffness is reduced by 24, 52, and 60%. In contrast, the reduction percentages for the yielding stiffness are 8, 12, and 16%. The initial stiffness is more affected by increasing the temperature values by twice those recorded for the yielding stiffness. This could explain that the onset of cracking is increased significantly by the occurrence of more cracks also widened. In contrast, creating an opening reduces the slab stiffness in both stages due to the reduction of concrete volume and rein amount of reinforcement. As a result of increasing the opening ratio, the initial stiffness values were degraded by 19, 47, and 55% compared to 30, 55, and 62% for the yielding stiffness at different opening ratios of 2.0, 4.5, and 8%, respectively. Moreover, it has been shown by Rambo et al. [46] that the elastic modulus and the concrete compressive strength are significantly reduced under the effect of high temperature.

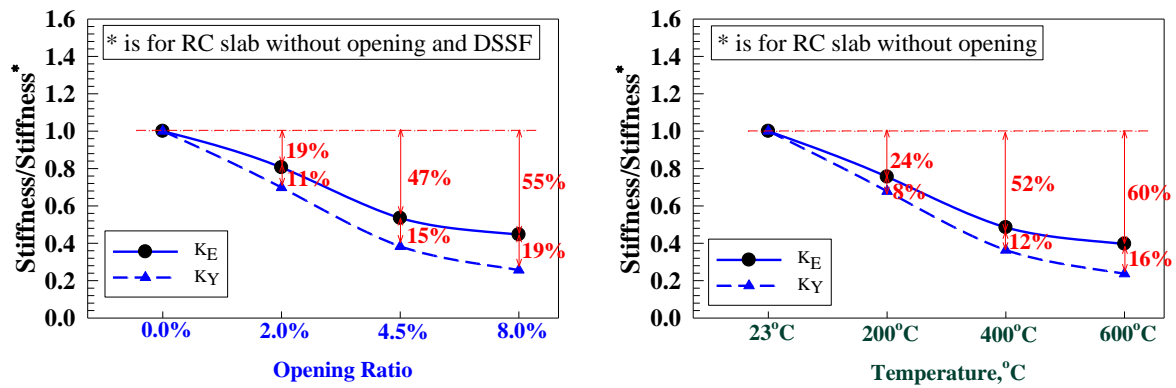


Figure 13. Normalized stiffness versus opening ratio and exposed temperature

#### 4.6. Ductility Index

Ductility is the structure's capability to undergo an inelastic deformation without losing its load resistance properties. Ductility is measured in this study using two main measures: displacement ( $\mu_{\Delta}$ ) and energy absorption ( $\mu_{EA}$ ), as shown in Table 5. Generally, the dispersion of discrete fibers into concrete material reduces the concrete weakness in tension. Thus, ductility and toughness values are improved [47].

##### 4.6.1. Displacement Ductility Index

The displacement ductility index is the ratio between the displacement at failure and the displacement at yielding. Figure 14 shows the effect of different opening ratios and DSSF material under different elevated temperatures. Values were normalized with respect to (ST23O0F0) specimen; a slab without an opening or DSSF material tested at room temperature. Figure 14 shows an approximately linear relationship between the normalized ductility index, opening size ratio, and temperature value. Generally, duplicating the opening size generally enhances the ductility index value by a maximum improvement percentage of 13% under an opening of size ratio of less than 4.5%. Moreover, the improvement percentage becomes less under a further increase in the opening size ratio. Furthermore, duplicating the temperature reduced the slab's ductility by an average value of 15%. Nana et al. [48] reported that FRC has higher ductility values compared to conventionally reinforced concrete. Moreover, crack distribution is intensified but with smaller crack opening values.

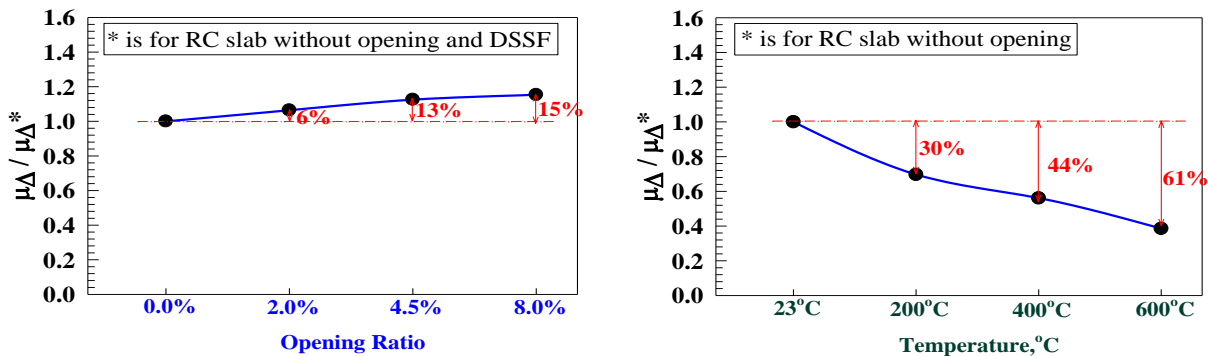


Figure 14. Normalized displacement ductility versus opening ratio and exposed temperature

##### 4.6.2. Energy Absorption Ductility Index

The energy absorption capacity (EA) was calculated as the area under the load-deflection curve. Both yielding and ultimate energy absorption values were calculated as shown in Table 5. The presented results showed that temperature increase causes the energy absorption value to decrease in their yielding and ultimate measures. In contrast, the energy capability increases under different opening ratios. Figure 15 shows an increasingly linear relationship between the energy absorption and the opening ratio. The improvement percentage varies between 6 and 34%. Meanwhile, an inversely linear relationship exists between energy absorption and temperature. The reduction percentages range from 24 and 77%. This confirmed the reported conclusion in the literature that the energy absorption capability is generally increased when fibers are added to the concrete mix [49-51]. Moreover, FRC is proven to have higher toughness values compared to ordinary concrete [47, 52].

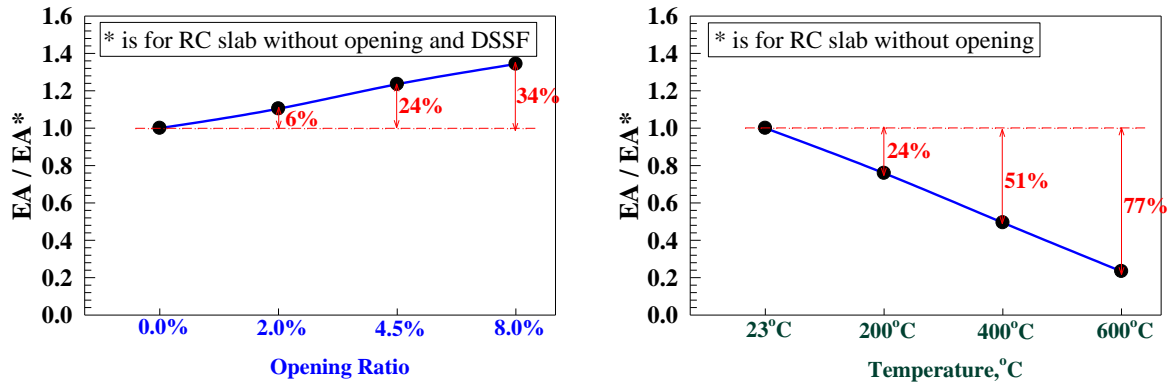
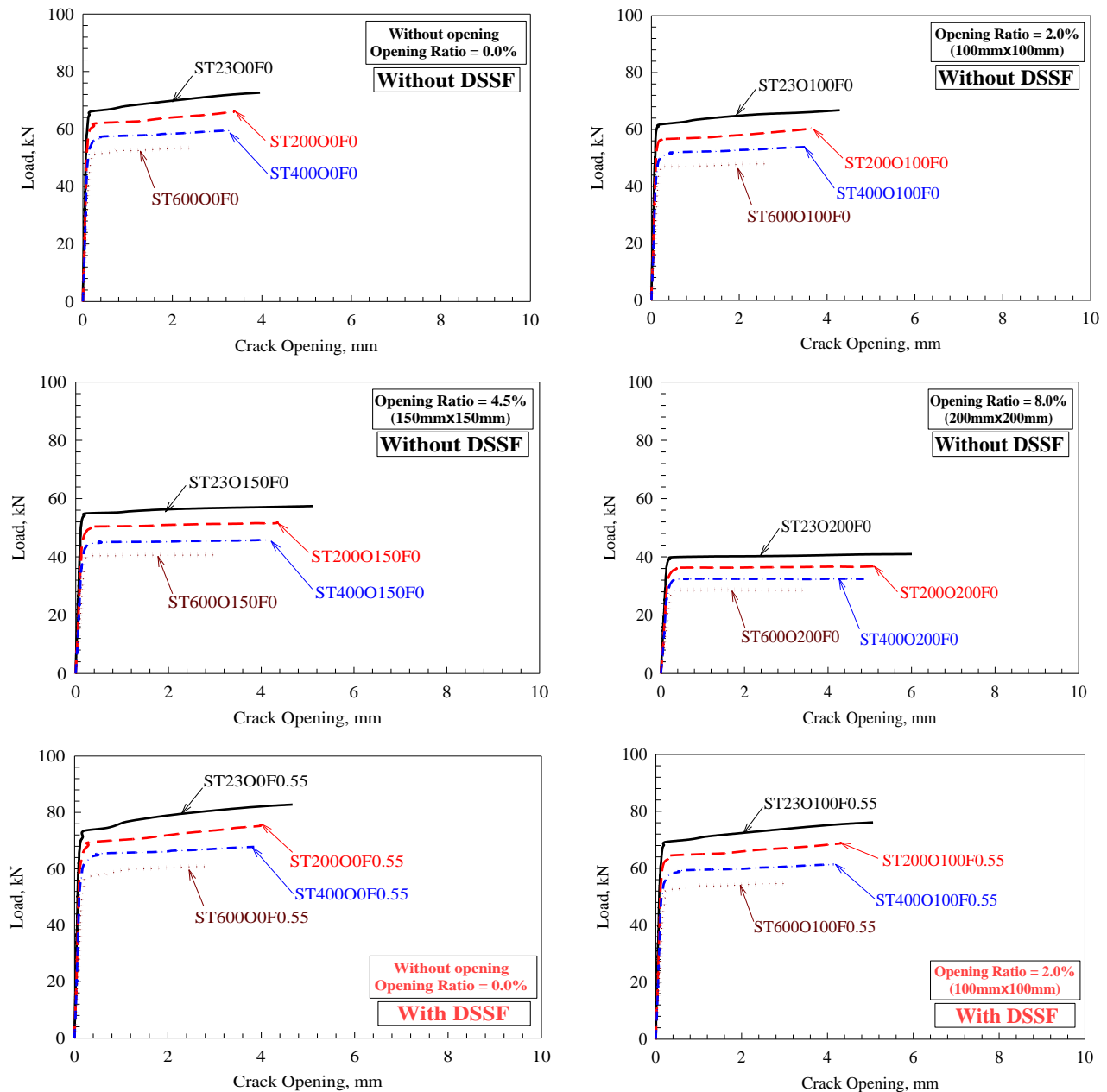


Figure 15. Normalized energy absorption ductility versus opening ratio and exposed temperature

#### 4.7. Load versus Crack Opening Behavior

Figure 16 represents the load and crack opening relationship for all the slabs. Crack width was calculated by fixing a 150 mm length between the transducers in their position and measuring their locations before and after testing.



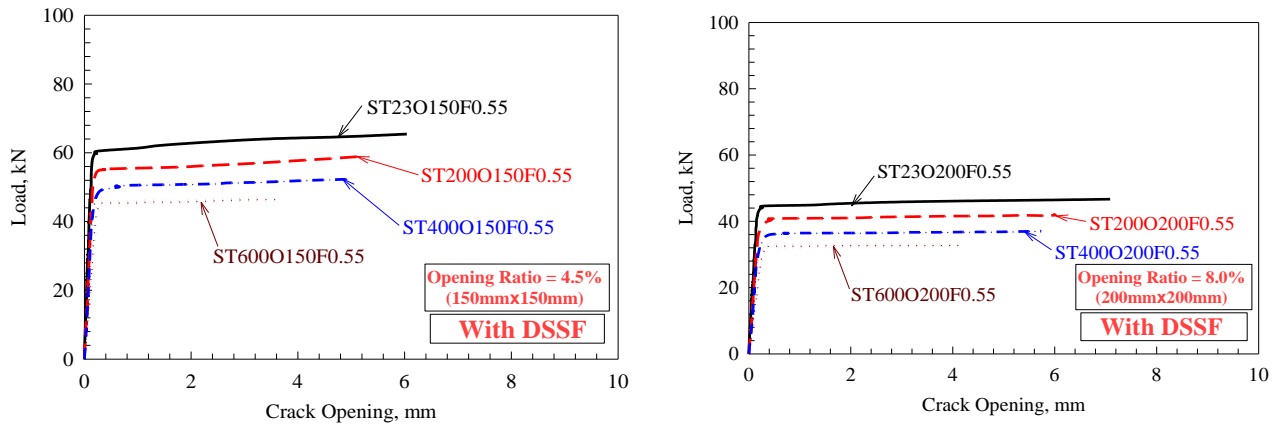


Figure 16. Load versus crack opening curves

The recorded crack width values are illustrated in Table 4. In addition, crack opening behavior is presented in Figure 16. The two measures are additional evidence of the feasibility of DSSF in providing the internal structure with more stability even at high deflection values. Generally, the crack stabilization in control cracking behavior is increased by 8, 29, and 52% for the different opening ratios normalized with respect to a slab without an opening having an added load at a one mm wide crack. Furthermore, increasing the temperature reduces the required load to cause a 1 mm crack width by 15, 28, and 39% at temperatures of 200, 400, and 600°C, respectively. Furthermore, Carnovale and Vecchio [43] stated that cracks are stabilized within the DSSF strengthened concrete, and an increase in the residual load occurs even at large crack widths. Previously, it was reported that the relationship between the stress and the crack width was presented as an exploration of the post-cracking behavior of the DSSF strengthened concrete, which can be extracted directly using a uniaxial tensile testing procedure [53] or indirectly by bending test.

## 5. Conclusion

Based on the previous investigation into the effect of DSSF on the flexural performance of one-way slabs, adding the DSSF material significantly improves the tensile strength and modulus of elasticity of concrete, whereas the compressive strength is not affected. Moreover, improvements occur in the cracking and ultimate load, cracking width, cracking and yielding stiffnesses, and cracking mechanism. This can be interpreted by the high tensile strength and toughness of the hybrid concrete, besides its internal stability, which resulted in the ductile and stable behavior of slabs with DSSF. Furthermore, a square opening causes the overall slab's capability to be significantly reduced compared to those without an opening due to the resulting stress concentration and crack intensification within the opening region. In addition, for DSSF strengthened slabs, increasing the opening ratio to twice the time causes the ultimate deflection to be increased by 4% on average. Moreover, an increasing linear relationship exists between the applied load, the resulting deflection, the longitudinal concrete strain, and the steel reinforcement. Finally, the opening ratio and high temperature influence the elastic and yielding stiffnesses, where a noticeable reduction is observed under the effect of increasing those parameters. Generally, duplicating the opening size generally enhances the ductility index value by a maximum improvement percentage of 13% under an opening size ratio of less than 4.5%. Moreover, the improvement percentage becomes less under a further increase in the opening size ratio. Nevertheless, the initial stiffness is more affected by increasing the temperature values twice those recorded for the yielding stiffness.

## 6. Declarations

### 6.1. Data Availability Statement

The data presented in this study are available on request from the corresponding author.

### 6.2. Funding

The financial support was provided by the Deanship of Scientific Research at Jordan University of Science and Technology under Grant number 2022/341.

### 6.3. Acknowledgements

The author gratefully acknowledges the financial support from the Deanship of Scientific Research at Jordan University of Science and Technology under Grant number 2022/341.

### 6.4. Conflicts of Interest

The author declares no conflict of interest.

## 7. References

- [1] ACI 544.1R-96. Report on Fiber Reinforced Concrete. American Concrete Institute (ACI), Farmington Hills, United States.
- [2] Baran, E., & Arsava, T. (2012). Flexural strength design criteria for concrete beams reinforced with high-strength steel strands. *Advances in Structural Engineering*, 15(10), 1781–1792. doi:10.1260/1369-4332.15.10.1781.
- [3] Abdul-Ahad, R. B., & Aziz, O. Q. (1999). Flexural strength of reinforced concrete T-beams with steel fibers. *Cement and Concrete Composites*, 21(4), 263–268. doi:10.1016/s0958-9465(99)00009-8.
- [4] Altun, F., Haktanir, T., & Ari, K. (2007). Effects of steel fiber addition on mechanical properties of concrete and RC beams. *Construction and Building Materials*, 21(3), 654–661. doi:10.1016/j.conbuildmat.2005.12.006.
- [5] Campione, G., & Letizia Mangiavillano, M. (2008). Fibrous reinforced concrete beams in flexure: Experimental investigation, analytical modelling and design considerations. *Engineering Structures*, 30(11), 2970–2980. doi:10.1016/j.engstruct.2008.04.019.
- [6] Dancygier, A. N., & Savir, Z. (2006). Flexural behavior of HSFRC with low reinforcement ratios. *Engineering Structures*, 28(11), 1503–1512. doi:10.1016/j.engstruct.2006.02.005.
- [7] Chunxiang, Q., & Patnaikuni, I. (1999). Properties of high-strength steel fiber-reinforced concrete beams in bending. *Cement and Concrete Composites*, 21(1), 73–81. doi:10.1016/S0958-9465(98)00040-7.
- [8] Adom-Asamoah, M., & Kankam, C. K. (2009). Flexural behaviour of one-way concrete slabs reinforced with steel bars milled from scrap metals. *Materials and Design*, 30(5), 1737–1742. doi:10.1016/j.matdes.2008.07.048.
- [9] Swamy, R. N., & Sa'ad, A. (1981). Deformation and Ultimate Strength in Flexure of Reinforced Concrete Beams Made With Steel Fiber Concrete. *Journal of the American Concrete Institute*, 78(5), 395–405. doi:10.14359/10525.
- [10] Yang, J. M., Min, K. H., Shin, H. O., & Yoon, Y. S. (2012). Effect of steel and synthetic fibers on flexural behavior of high-strength concrete beams reinforced with FRP bars. *Composites Part B: Engineering*, 43(3), 1077–1086. doi:10.1016/j.compositesb.2012.01.044.
- [11] Azzawi, R., & Varughese, N. (2020). Flexural behavior of preflex sfrc-encased steel joist composite beams. *Results in Engineering*, 7, 100122. doi:10.1016/j.rineng.2020.100122.
- [12] Khalid, M. Y., Al Rashid, A., Arif, Z. U., Sheikh, M. F., Arshad, H., & Nasir, M. A. (2021). Tensile strength evaluation of glass/jute fibers reinforced composites: An experimental and numerical approach. *Results in Engineering*, 10, 100232. doi:10.1016/j.rineng.2021.100232.
- [13] Khalid, M. Y., Al Rashid, A., Arif, Z. U., Ahmed, W., Arshad, H., & Zaidi, A. A. (2021). Natural fiber reinforced composites: Sustainable materials for emerging applications. *Results in Engineering*, 11, 100263. doi:10.1016/j.rineng.2021.100263.
- [14] Al-Rousan, R. Z. (2018). Behavior of macro synthetic fiber concrete beams strengthened with different CFRP composite configurations. *Journal of Building Engineering*, 20, 595–608. doi:10.1016/j.jobe.2018.09.009.
- [15] Enochsson, O., Lundqvist, J., Täljsten, B., Rusinowski, P., & Olofsson, T. (2007). CFRP strengthened openings in two-way concrete slabs - An experimental and numerical study. *Construction and Building Materials*, 21(4), 810–826. doi:10.1016/j.conbuildmat.2006.06.009.
- [16] Asadei, P., Ibell, T., & Nanni, A. (2003). Experimental results of one-way slabs with openings strengthened with CFRP laminates. *Fibre-Reinforced Polymer Reinforcement for Concrete Structures*. doi:10.1142/9789812704863\_0105.
- [17] ACI 318-14. (2014). Building Code Requirements for Structural Concrete and Commentary. American Concrete Institute (ACI), Farmington Hills, United States.
- [18] di Prisco, M., Plizzari, G., & Vandewalle, L. (2009). Fibre reinforced concrete: new design perspectives. *Materials and Structures*, 42(9), 1261–1281. doi:10.1617/s11527-009-9529-4.
- [19] Sorelli, L. G., Meda, A., & Plizzari, G. A. (2006). Steel fiber concrete slabs on ground: a structural matter. *ACI Materials Journal*, 103(4), 551. doi:10.14359/16431.
- [20] Mobasher, B., Yao, Y., & Soranakom, C. (2015). Analytical solutions for flexural design of hybrid steel fiber reinforced concrete beams. *Engineering Structures*, 100, 164–177. doi:10.1016/j.engstruct.2015.06.006.
- [21] Barros, J. A. O., Taheri, M., & Salehian, H. (2015). A model to simulate the moment-rotation and crack width of FRC members reinforced with longitudinal bars. *Engineering Structures*, 100, 43–56. doi:10.1016/j.engstruct.2015.05.036.
- [22] Pujadas, P., Blanco, A., De La Fuente, A., & Aguado, A. (2012). Cracking behavior of FRC slabs with traditional reinforcement. *Materials and Structures*, 45(5), 707–725. doi:10.1617/s11527-011-9791-0.
- [23] Minelli, F., & Plizzari, G. A. (2013). On the effectiveness of steel fibers as shear reinforcement. *ACI Structural Journal*, 110(3), 379–389. doi:10.14359/51685596.

- [24] Hawkins, N. M., & Mitchell, D. (1979). Progressive Collapse of Flat Plate Structures. *CI Journal Proceedings*, 76(7), 775–808. doi:10.14359/6981.
- [25] Mitchell, D., & Cook, W. D. (1984). Preventing Progressive Collapse of Slab Structures. *Journal of Structural Engineering*, 110(7), 1513–1532. doi:10.1061/(asce)0733-9445(1984)110:7(1513).
- [26] Michels, J., Waldmann, D., Maas, S., & Zürbes, A. (2012). Steel fibers as only reinforcement for flat slab construction - Experimental investigation and design. *Construction and Building Materials*, 26(1), 145–155. doi:10.1016/j.conbuildmat.2011.06.004.
- [27] Michels, J., Christen, R., & Waldmann, D. (2013). Experimental and numerical investigation on post-cracking behavior of steel fiber reinforced concrete. *Engineering Fracture Mechanics*, 98(1), 326–349. doi:10.1016/j.engfracmech.2012.11.004.
- [28] Pujadas, P., Blanco, A., Cavalaro, S., & Aguado, A. (2014). Plastic fibres as the only reinforcement for flat suspended slabs: Experimental investigation and numerical simulation. *Construction and Building Materials*, 57, 92–104. doi:10.1016/j.conbuildmat.2014.01.082.
- [29] Destrée, X. (2008). Free suspended elevated slabs of steel fibre reinforced concrete: full scale test results and design. 941-950, 7<sup>th</sup> International symposium of fiber-reinforced concrete: design and applications BEFIB, 17-19 September, 2008, Chennai, India.
- [30] RILEM TC 162-TDF. (2003). Test and design methods for steel fibre reinforced concrete. *Materials and Structures*, 36, 560-567.
- [31] Alrawashdeh, A., & Eren, O. (2022). Mechanical and physical characterisation of steel fibre reinforced self-compacting concrete: Different aspect ratios and volume fractions of fibres. *Results in Engineering*, 13, 100335. doi:10.1016/j.rineng.2022.100335.
- [32] Gapsari, F., Djakfar, L., Handajani, R. P., Yusran, Y. A., Hidayatullah, S., Suteja, Rangappa, S. M., & Siengchin, S. (2022). The application of timoho fiber coating to improve the composite performance. *Results in Engineering*, 15, 100499. doi:10.1016/j.rineng.2022.100499.
- [33] Roesler, J. R., Altoubat, S. A., Lange, D. A., Rieder, K. A., & Ulrich, G. R. (2006). Effect of synthetic fibers on structural behavior of concrete slabs-on-ground. *ACI Materials Journal*, 103(1), 3–10. doi:10.14359/15121.
- [34] Attari, N., Amziane, S., & Chemrouk, M. (2012). Flexural strengthening of concrete beams using CFRP, GFRP and hybrid FRP sheets. *Construction and Building Materials*, 37, 746–757. doi:10.1016/j.conbuildmat.2012.07.052.
- [35] Kara, I. F., Ashour, A. F., & Köroğlu, M. A. (2015). Flexural behavior of hybrid FRP/steel reinforced concrete beams. *Composite Structures*, 129, 111–121. doi:10.1016/j.compstruct.2015.03.073.
- [36] Ababneh, A., Al-Rousan, R., Alhassan, M., & Alqadami, M. (2017). Influence of synthetic fibers on the shear behavior of lightweight concrete beams. *Advances in Structural Engineering*, 20(11), 1671–1683. doi:10.1177/1369433217691773.
- [37] Al-Rousan, R. Z. (2018). Empirical and NLFEA prediction of bond-slip behavior between DSSF concrete and anchored CFRP composites. *Construction and Building Materials*, 169, 530–542. doi:10.1016/j.conbuildmat.2018.03.013.
- [38] Al-Rousan, R. Z., Alhassan, M. A., & AlShuqari, E. A. (2018). Behavior of plain concrete beams with DSSF strengthened in flexure with anchored CFRP sheets—Effects of DSSF content on the bonding length of CFRP sheets. *Case Studies in Construction Materials*, 9, 195. doi:10.1016/j.cscm.2018.e00195.
- [39] Amin, A., Foster, S. J., Gilbert, R. I., & Kaufmann, W. (2017). Material characterisation of macro synthetic fibre reinforced concrete. *Cement and Concrete Composites*, 84, 124–133. doi:10.1016/j.cemconcomp.2017.08.018.
- [40] Mathews, M. E., Kiran, T., Hasa Naidu, V. C., Jeyakumar, G., & Anand, N. (2020). Effect of high-temperature on the mechanical and durability behaviour of concrete. *Materials Today: Proceedings*, 42, 718–725. doi:10.1016/j.matpr.2020.11.153.
- [41] Serafini, R., Dantas, S. R. A., Salvador, R. P., Agra, R. R., Rambo, D. A. S., Berto, A. F., & de Figueiredo, A. D. (2019). Influence of fire on temperature gradient and physical-mechanical properties of macro-synthetic fiber reinforced concrete for tunnel linings. *Construction and Building Materials*, 214, 254–268. doi:10.1016/j.conbuildmat.2019.04.133.
- [42] Far, H., & Nejadi, S. (2021). Experimental investigation on interface shear strength of composite PVC encased macro-synthetic fibre reinforced concrete walls. *Structures*, 34, 729–737. doi:10.1016/j.istruc.2021.08.008.
- [43] Carnovale, D., & Vecchio, F. J. (2014). Effect of fiber material and loading history on shear behavior of fiber-reinforced concrete. *ACI Structural Journal*, 111(5), 1235–1244. doi:10.14359/51686809.
- [44] Srikar, G., Anand, G., & Suriya Prakash, S. (2016). A Study on Residual Compression Behavior of Structural Fiber Reinforced Concrete Exposed to Moderate Temperature Using Digital Image Correlation. *International Journal of Concrete Structures and Materials*, 10(1), 75–85. doi:10.1007/s40069-016-0127-x.
- [45] Bažant, Z. P., & Kaplan, M. F. (1996). *Concrete at high temperatures: material properties and mathematical models*. Longman Group Limited, London, United Kingdom.

- [46] Rambo, D. A. S., Blanco, A., Figueiredo, A. D. de, Santos, E. R. F. dos, Toledo, R. D., & Gomes, O. da F. M. (2018). Study of temperature effect on macro-synthetic fiber reinforced concretes by means of Barcelona tests: An approach focused on tunnels assessment. *Construction and Building Materials*, 158, 443–453. doi:10.1016/j.conbuildmat.2017.10.046.
- [47] Walraven, J. C. (2009). High performance fiber reinforced concrete: Progress in knowledge and design codes. *Materials and Structures/Materiaux et Constructions*, 42(9), 1247–1260. doi:10.1617/s11527-009-9538-3.
- [48] Nana, W. S. A., Tran, H. V., Goubin, T., Kubisztal, G., Bennani, A., Bui, T. T., Cardia, G., & Limam, A. (2021). Behaviour of macro-synthetic fibers reinforced concrete: Experimental, numerical and design code investigations. *Structures*, 32, 1271–1286. doi:10.1016/j.istruc.2021.03.080.
- [49] Richardson, A., & Coventry, K. (2015). Dovetailed and hybrid synthetic fibre concrete - Impact, toughness and strength performance. *Construction and Building Materials*, 78, 439–449. doi:10.1016/j.conbuildmat.2015.01.003.
- [50] Richardson, A., Coventry, K., Lamb, T., & Mackenzie, D. (2016). The addition of synthetic fibres to concrete to improve impact/ballistic toughness. *Construction and Building Materials*, 121, 612–621. doi:10.1016/j.conbuildmat.2016.06.024.
- [51] Gopalaratnam, V. S., & Gettu, R. (1995). On the characterization of flexural toughness in fiber reinforced concretes. *Cement and Concrete Composites*, 17(3), 239–254. doi:10.1016/0958-9465(95)99506-O.
- [52] Shah, S. P., & Rangan, B. V. (1971). Closure to “Effects of Reinforcements on Ductility of Concrete.” *Journal of the Structural Division*, 97(10), 2604–2604. doi:10.1061/jsdeag.0003029.
- [53] Foster, S. J. (2014). FRC design according to the draft Australian bridge code. *Proceedings FRC 2014 Joint ACI-fib International Workshop Fibre Reinforced Concrete: From Design to Structural Applications*, 24-25 July 2014, Polytechnique Montreal, Montreal, Canada.